Spectrochimica Acta Part A: Molecular and Biomolecular Spectroscopy 224 (2020) 117467

Contents lists available at ScienceDirect

Spectrochimica Acta Part A: Molecular and Biomolecular Spectroscopy

journal homepage: www.elsevier.com/locate/saa

Rhodol-based fluorescent probes for the detection of fluoride ion and its application in water, tea and live animal imaging

Xilang Jin [a,1], Jingkai Gao [b,1], Ting Wang [a], Wan Feng [a], Rong Li [c], Pu Xie [a], Lele Si [a], Hongwei Zhou [a,*], Xianghan Zhang [b,**]

[a] School of Materials and Chemical Engineering, Xi'an Technological University, Xi'an 710032, Shaanxi, China
[b] School of Life Sciences and Technology, Xidian University, Xi'an 710071, Shaanxi, China
[c] Hancheng Hongda Sichuan Pepper Flavor Co., Ltd, Hancheng 715400, Shaanxi, China

ARTICLE INFO

Article history:
Received 21 February 2019
Received in revised form 23 July 2019
Accepted 10 August 2019
Available online 11 August 2019

Keywords:
Fluoride ion
Fluorescent
Seminaphthorhodafluor dye
Tea samples
Bioimaging

ABSTRACT

Herein, we presented two novel turn-on colorimetric and fluorescent probes based on a F^- triggered Si—O bond cleavage reaction, which displayed several desired properties for the quantitative detection for F^-, such as high specificity, rapid response time (within 3 min) and naked-eye visualization. The fluorescence intensity at 574 nm (absorbance at 544 nm) of the solution was found to increase linearly with the concentration of F^- (0.00–30.0 μM) with the detection limit was estimated to be 0.47 μM/0.48 μM. Based on these excellent optical properties, the probes were employed to monitor F^- in real water samples and tea samples with satisfactory. Furthermore, it was successfully applied for fluorescent imaging of F^- in living nude mice, suggesting that it could be used as a powerful tool to predict and explore the biological functions of F^- in physiological and pathological processes.

1. Introduction

As the smallest anion distributed in nature, inorganic fluoride ion (F^-) which mainly derived from foodstuffs and groundwater exerts a great influence on human health particularly in preventing dental caries [1–3]. Nevertheless, excessive ingestion of fluoride ion may result in fluorosis, urolithiasis, skeletal disease and even lead to cancers [4–6]. For these reasons, the controlled consumption of fluoride in the human body is a serious concern throughout the world [7,8]. Therefore, it is very meaningful to develop a convenient and efficient technique for the detection and quantification of fluoride ions in real samples and complicated biological systems.

Compared with the traditional sophisticated analytical techniques (ion chromatography, reversed-phase high-performance liquid chromatography, ^{19}F NMR, fluoride ion selective electrode), molecular probe-based fluorometric and colorimetric methodology [9–17] has been employed as a powerful technology to track cations, anions and biological molecules *in vitro* and *in vivo* for its high specificity, high sensitivity, real-time imaging and noninvasive monitoring capability [18–26]. Accordingly, numerous turn-on fluorescent molecular probes for monitoring F^- containing common fluorophores including rhodamine, coumarin, tetrahydroxanthenone, calix[4]crown and naphthalimide have been rapidly constructed in recent years [27–37]. Moreover, reports on rhodol-based (a special combination structure of rhodamine and fluorescein) fluorescent probes for the detecting of F^- are scarce. Rhodol dyes are excellent candidates for fluorescent probes which have the advantages, such as excellent optical features, high extinction coefficients, high photo-stability, long wavelength absorption and emission [38–41]. Therefore, the suitable design of a novel rhodol-based fluorescent probe that could selectively responds to F^- in real samples and *in vivo* is still a challenge for the analytical chemists.

Herein, we constructed an unprecedented example (Scheme 1) of a highly sensitive, F^--selective colorimetric and fluorometric rhodol-based probe which consisted seminaphthorhodafluor dye (chromophore) and tert-butyl dimethyl chlorosilane/tert-butyl diphenyl chlorosilane (recognition site of F^-). Furthermore, probe **1** exhibits ideal fluorometric and colorimetric properties and exhibited desirable selectivity to F^- in real samples and *in vivo*.

2. Experimental

2.1. Materials and methods

All chemicals were purchased from commercial suppliers and used without further purification. UV–Vis absorption and fluorescence

* Corresponding author.
** Correspondence to: X. Zhang, School of Materials and Chemical Engineering, Xi'an Technological University, Xi'an 710032, Shaanxi, China.
E-mail addresses: xatuzhou@163.com (H. Zhou), jinxilang_911@163.com, xhzhang@xidian.edu.cn (X. Zhang).
[1] Xilang Jin and Jingkai Gao contributed equally to this work.

https://doi.org/10.1016/j.saa.2019.117467
1386-1425/

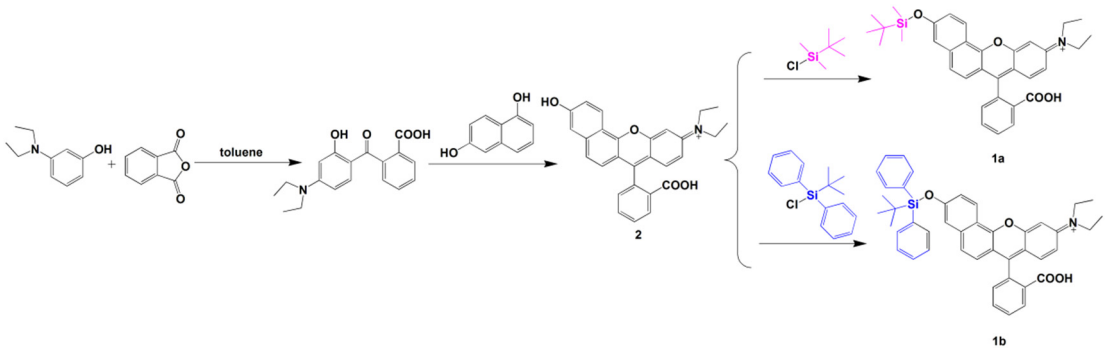

Scheme 1. Synthesis route of probe **1**.

spectra were performed on Shimadzu UV-1700 spectrophotometer and Hitachi F-4500 fluorescence spectrophotometer (excitation and emission slits set at 5.0 nm), respectively. High-resolution mass spectra (HR-MS) were measured by a Brukermicro TOF-QII ESI-Q-TOF LC/MS/MS Spectrometer. ^{1}H NMR spectra were recorded on a Varian INOVA-400 MHz spectrometer using tetramethylsilane as internal standard. *In vivo* fluorescence imaging analysis was carried out in an IVIS Kinetic imaging system.

2.2. General procedure

The stock solution of probe **1** (1 mM) was prepared in DMSO. The solutions of biologically relevant analytes stock solutions (1 mM) were prepared in deionized water. For all measurements, the absorbance was recorded at 544 nm and the fluorescence intensity was recorded at 574 nm (λex = 500 nm).

2.3. Synthesis of probes 1a and 1b

Seminaphthorhodafluor dye (compound **2**) was synthesized according to the reported procedures [40].

^{1}H NMR(Chloroform *d*, 400 MHz): δ (ppm) 1.16 (t, *J* = 7.0 Hz, 6H), 3.33 (q, *J* = 7.2 Hz, 4H), 5.32 (s, 1H), 6.44 (dd, *J* = 9.3, 2.5 Hz, 1H), 6.58 (d, *J* = 2.6 Hz, 1H), 6.72 (d, *J* = 8.8 Hz, 1H), 6.87 (d, *J* = 9.0 Hz, 1H), 6.95 (d, *J* = 2.4 Hz, 1H), 7.01 (d, *J* = 8.8 Hz, 1H), 7.09 (dd, *J* = 9.1, 2.4 Hz, 1H), 7.15 (m, 1H), 7.62 (tt, *J* = 7.3, 5.8 Hz, 2H), 8.15 (m, 1H), 8.25 (d, *J* = 9.0 Hz, 1H). MS (ESI) *m*/*z* = 438.1715 $[M]^+$, calc. for $C_{28}H_{24}NO_4^+$ = 438.1700.

A solution of tert-butyl dimethyl chlorosilane/tert-butyl diphenyl chlorosilane (11.0 mmol) and imidazole (1.50 g, 22.0 mmol) in anhydrous CH_2Cl_2 (10 mL) was added dropwise to a solution of compound 2 (4.38 g, 10.0 mmol) in CH_2Cl_2 (30 mL) at 0 °C for 30 min. The solution was warmed to room temperature and stirred for 3 h. Then the resultant residue was washed with H_2O (50 mL) and dried over anhydrous Na_2SO_4. The residue was concentrated and purified by column chromatography (CH_3OH/CH_2Cl_2 = 1/250).

Probe **1a**: light pink powder, 3.12 g, yield: 56.52%. ^{1}H NMR(DMSO d_6, 400 MHz): δ (ppm) 0.31 (s, 6H), 1.04 (s, 9H), 1.17 (t, *J* = 7.0 Hz, 6H), 3.45(q, *J* = 6.8 Hz, 4H), 6.58 (m, 2H), 6.70 (d, *J* = 8.8 Hz, 1H), 6.78 (d, *J* = 2.3 Hz, 1H), 7.33 (m, 2H), 7.38 (d, *J* = 2.4 Hz, 1H), 7.53 (d, *J* = 8.7 Hz, 1H), 7.81 (m, 2H), 8.08 (d, *J* = 7.5 Hz, 1H), 8.54 (d, *J* = 9.0 Hz, 1H). MS (ESI) *m*/*z* = 552.2547 [M], calc. for $C_{34}H_{38}NO_4$ Si = 552.2565.

Probe **1b**: light pink powder, 3.03 g, yield: 44.82%. ^{1}H NMR (Chloroform *d*, 400 MHz): δ (ppm) 1.24 (m, 6H), 1.27 (m, 9H), 3.75 (q, *J* = 7.0 Hz, 4H), 6.63 (d, *J* = 8.8 Hz, 3H), 7.05 (d, *J* = 2.4 Hz, 1H), 7.10 (d, *J* = 8.8 Hz, 1H), 7.15 (dd, *J* = 6.6, 1.8 Hz, 2H), 7.39 (td, *J* = 7.1, 6.6, 1.7 Hz, 5H), 7.44 (m, 2H), 7.55 (dd, *J* = 5.7, 3.3 Hz, 1H), 7.63 (m, 2H), 7.77 (dt, *J* = 8.0, 1.2 Hz, 4H), 8.05 (m, 1H), 8.39 (d, *J* = 9.1 Hz, 1H). MS (ESI) *m*/*z* = 676.2967 [M], calc. for $C_{44}H_{42}NO_4Si$ = 676.2878.

3. Results and discussion

3.1. Optical properties of probe 1a

With probe **1a** and **1b** in hands, F^--mediated fluorescence and absorption responses were initially investigated in DMSO-PBS (5/95, v/v,

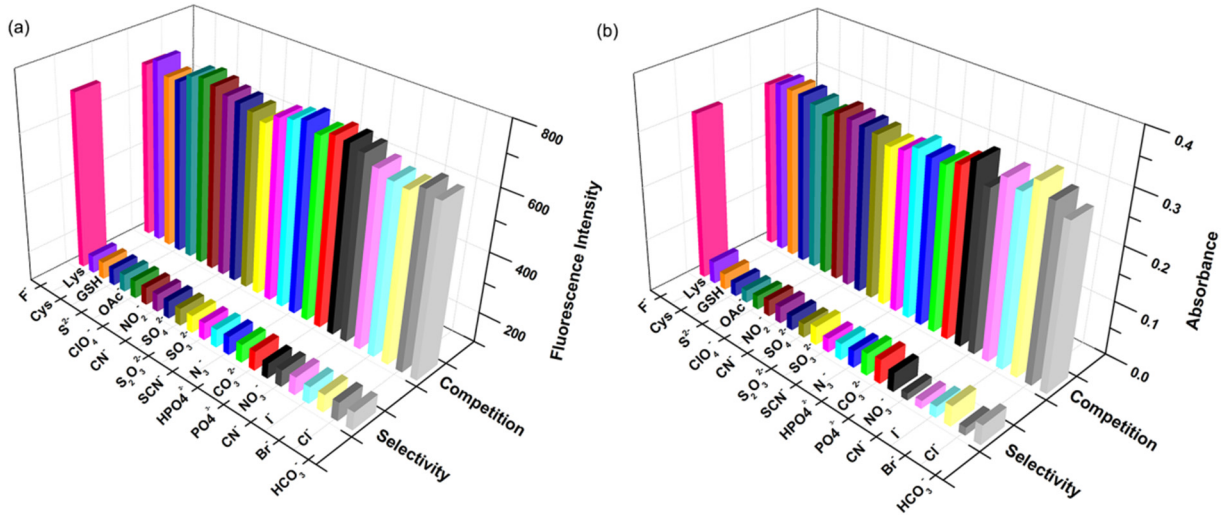

Fig. 1. Fluorescence responses (574 nm)/absorption responses (544 nm) of probe **1a** (10.0 μM) to various interfering species. The pillars in the front row: probe **1a** treated with the interfering species (1000 μM). The pillars in the back row: probe **1a** treated with the interfering species (1000 μM) followed by F^- (20.0 μM). (λ_{ex} = 500 nm, silt = 5 nm/5 nm).

Table 1
Application of the probe **1a** in determination of F^- in tea samples.

Sample	Filtrate I (μmol/L)	F^- spiked (μmol/L)	F^- recovered mean[a] ± SD[b] (μmol/L)	Recovery (%)
Black Tea (Puer Tea)	9.88	5.00	15.11 ± 0.32	101.5
		10.00	20.03 ± 0.32	100.8
		15.00	25.55 ± 0.26	99.3
Green Tea (Jintan Queshe)	4.12	5.00	9.01 ± 0.18	98.7
		10.00	14.22 ± 0.29	100.7
		15.00	19.35 ± 0.31	101.2

[a] Mean of three determination.
[b] SD: standard deviation.

pH 7.4) solution. The results suggested that the R moiety (tert-butyl dimethyl-, tert-butyl diphenyl-) had no significant impact on the spectral properties. Hence, only probe **1a** was discussed in this article and the spectral properties of probe **1b** was shown in the supporting information.

As shown in Fig. 1, the optical responses of probe **1a** towards a variety of biologically relevant species were examined. Upon the addition of various analytes (HCO_3^-, Cl^-, Br^-, I^-, CN^-, NO_3^-, PO_4^{3-}, CO_3^{2-}, HPO_4^{2-}, SCN^-, N_3^-, SO_3^{2-}, HSO_3^-, $S_2O_3^{2-}$, SO_4^{2-}, NO_2^-, ClO_4^-, OAc^-, S^{2-}, GSH, Cys, Lys, 1.00 mM), only F^- induced a noticeable change in the fluorescence and absorption signals, no other interfering species had this effect. Moreover, the spectral response of probe **1a** towards F^- was not affected in the presence of other interfering relevant analytes (Table 1).

In the subsequent titration experiment (Fig. S1), the solution exhibited a prominent red fluorescence ($\Phi = 0.15$) and the fluorescence intensity at 574 nm (absorbance at 544 nm) of the solution was found to increase linearly with the concentration of F^- (0.00–30.0 μM, Fig. 2) with the detection limit was estimated to be 0.50 μM. The regression equation was $y = 22.995x + 201.26$ ($R^2 = 0.9865$) / $y = 0.0133x + 0.036$ ($R^2 = 0.9981$). These results showed that probe **1a** could be used to measure F^- quantitatively and qualitatively. Time-based fluorescence of probe **1a** with F^- reached its plateau within 3 min, indicating a rapid response of probe **1a** towards F^- (Figs. S3–4). Taking all these results together, probe **1a** displayed a great potential tool for the detection of F^- by the colorimetric and fluorometric dual mode.

3.2. Sensing mechanism studies

Taking consideration from previous literature [42,43], the proposed reaction mechanism was inferred as Scheme 2. Once attacked by F^-, probe **1a** underwent the deprotection mechanism by the cleavage of the Si—O bond (tert-butyl dimethyl- group). In order to further demonstrate the reaction mechanism, our probe was treated with 20 equiv. of F^-, the reaction mixture was purified and the corresponding product was characterized by HRMS and ^1H NMR. A new peak was observed at *m/z* 438.1614 (Fig. S23), which was assigned to compound **1a + F^-** $[M]^+$ (*m/z*, calcd: 438.1700). Meanwhile, the ^1H NMR spectral (Figs. S8, S20) strongly support the supposition that the F^--triggered cleavage reaction causes the release of seminaphthorhodafluor dye.

3.3. Fluorescence detection of F^- in real sample

The adequate intake for F^- from all sources was determined to be 0.05 mg/day/kg body weight and the concentration of in tea infusions of different type of teas were 0.29–6.01 mg/L [3]. To further study the practicality of the present probe, it was applied to detect F^- in potable water sample (Xi'an Technological University) and different type of tea samples (Black Tea and Red Tea) qualitatively and quantitatively. All of the samples were analyzed by probe **1a** with or without additional F^- at concentration levels of 5.0 μM, 10.0 μM and 15.0 μM based the regression equation ($y = 22.995x + 201.26$ ($R^2 = 0.9865$), Fig. 2). The analysis results were represented in Table S1 and 1. The results indicated that probe **1a** effectively measured and recovered the concentrations of spiked F^-. Therefore, the experimental results suggested that our probe could suitably and quantitatively detected F^- in real samples without interference from other environmentally relevant analytes.

3.4. Visualization of F^- in vivo

Inspired by these desired fluorescence properties, the applicability of the probe for visualizing F^- *in vivo* was subsequently explored. The Athymic nude mice which were selected as our model was given skin-pop injections of probe **1a** (20.0 μM) and finally by the injection of F^- (50.0 μM) at the same region after 30 min. In virtue of the small animal imaging system with a 540 nm excitation laser and a 570 nm emission filter, we gained the real-time recording of fluorescence signal that generated from the Athymic nude mice (Fig. 3). The mouse injected with probe **1a** and F^- displayed a strong fluorescence with time indicating that probe **1a** could respond to F^-. The results further demonstrated that our probe could be capable of specifically imaging exogenous F^- *in vivo*.

4. Conclusions

In conclusion, we had designed and synthesized two novel probes for the detection of F^- based on a F^- triggered Si—O bond cleavage reaction. The probes exhibited high sensitivity, high selectivity, rapid response for F^-, and could be successfully applied for F^- detection in potable water and tea samples. Moreover, the probes had been further

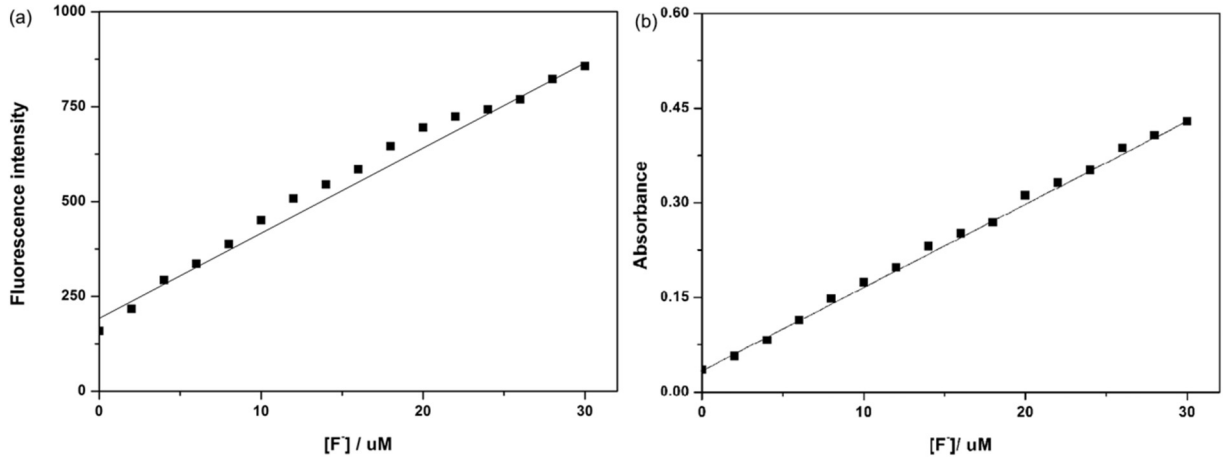

Fig. 2. The linear plots of fluorescence responses (574 nm)/absorption responses (544 nm) of probe **1a** (10.0 μM) upon addition of varied concentration of F^- (0.00–4.00 equvi.).

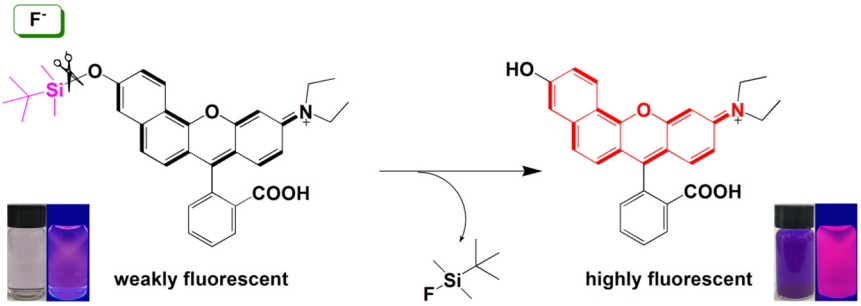

Scheme 2. Proposed mechanism for the detection of F^-.

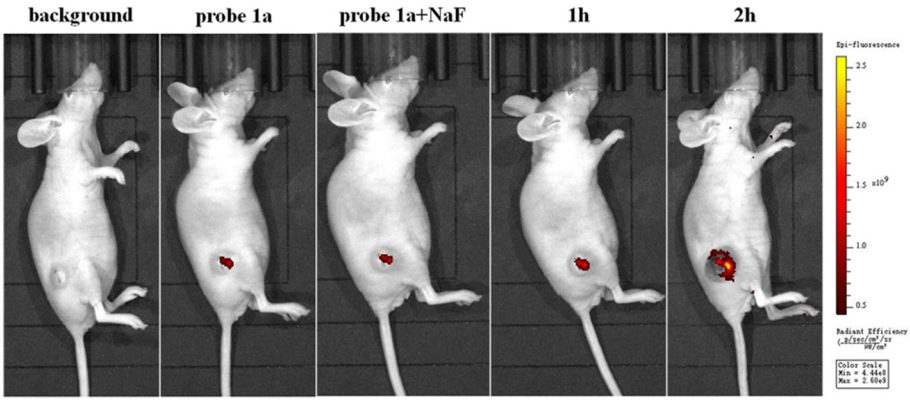

Fig. 3. Fluorescence images of exogenous NaF in Athymic nude mice.

utilized for fluorescence imaging of fluoride *in vivo* under physiological conditions.

Acknowledgements

The work was supported by the National Natural Science Foundation of China (No. 51603164, 21807085), the Natural Science Foundation Research Project of Shaanxi Province (No. 2018JQ2015), Scientific Research Program Funded by Shaanxi Provincial Education Department (No. 18JK0391).

Appendix A. Supplementary data

Supplementary data to this article can be found online at https://doi.org/10.1016/j.saa.2019.117467.

References

[1] S. Ayoob, A.K. Gupta, Fluoride in drinking water: a review on the status and stress effects, Crit. Rev. Environ. Sci. Technol. 36 (2006) 433–487.
[2] H.S. Horowitz, The 2001 CDC recommendations for using fluoride to prevent and control dental caries in the United States, J. Public Health Dent. 63 (2003) 3–8.
[3] A. Koblar, G. Tavčar, M. Ponikvar-Svet, Fluoride in teas of different types and forms and the exposure of humans to fluoride with tea and diet, Food Chem. 130 (2012) 286–290.
[4] M. Kleerekoper, The role of fluoride in the prevention of osteoporosis, Endocrinol. Metab. Clin. N. Am. 27 (1998) 441–452.
[5] B.D. Gessner, M. Beller, J.P. Middaugh, G.M. Whitford, Acute fluoride poisoning from a public water system, N. Engl. J. Med. 330 (1994) 95–99.
[6] P. Singh, M. Barjatiya, S. Dhing, R. Bhatnagar, S. Kothari, V. Dhar, Evidence suggesting that high intake of fluoride provokes nephrolithiasis in tribal populations, Urol. Res. 29 (2001) 238–244.
[7] B. Ke, W. Wu, L. Wei, F. Wu, G. Chen, G. He, M. Li, Cell and in vivo imaging of fluoride ion with highly selective bioluminescent probes, Anal. Chem. 87 (2015) 9110–9113.
[8] D. Wu, A.C. Sedgwick, T. Gunnlaugsson, E.U. Akkaya, J. Yoon, T.D. James, Fluorescent chemosensors: the past, present and future, Chem. Soc. Rev. 46 (2017) 7105–7123.
[9] X. Zhang, B. Wang, N. Zhao, Z. Tian, Y. Dai, Y. Nie, J. Tian, Z. Wang, X. Chen, Improved tumor targeting and longer retention time of NIR fluorescent probes using bioorthogonal chemistry, Theranostics 7 (2017) 3794–3802.
[10] X. Zhang, B. Wang, Y. Xia, S. Zhao, Z. Tian, P. Ning, Z. Wang, In vivo and in situ activated aggregation-induced emission probes for sensitive tumor imaging using tetraphenylethene-functionalized Trimethincyanines-encapsulated liposomes, ACS Appl. Mater. Interfaces 10 (2018) 25146–25153.
[11] J.M. Goldberg, F. Wang, C.D. Sessler, N.W. Vogler, D.Y. Zhang, W.H. Loucks, T. Tzounopoulos, S.J. Lippard, Photoactivatable sensors for detecting mobile zinc, J. Am. Chem. Soc. 140 (2018) 2020–2023.
[12] P. Cheng, J. Zhang, J. Huang, Q. Miao, C. Xu, K. Pu, Near-infrared fluorescence probes to detect reactive oxygen species for keloid diagnosis, Chem. Sci. 9 (2018) 6340–6347.
[13] D. Li, Z. Li, W. Chen, X. Yang, Imaging and detection of carboxylesterase in living cells and zebrafish pretreated with pesticides by a new near-infrared fluorescence off–on probe, J. Agric. Food Chem. 65 (2017) 4209–4215.
[14] H. Wang, J. Wang, S. Yang, H. Tian, Y. Liu, B. Sun, Highly selective and rapidly responsive fluorescent probe for hydrogen sulfide detection in wine, Food Chem. 257 (2018) 150–154.
[15] S. Dalapati, M.A. Alam, S. Jana, N. Guchhait, Naked-eye detection of F— and AcO— ions by Schiff base receptor, J. Fluor. Chem. 132 (2011) 536–540.
[16] S. Wang, Y. Zhao, C. Zhao, L. Liu, S. Yu, A colorimetric chemosensor for fluoride ions based on an indigo derivative, J. Fluor. Chem. 156 (2013) 236–239.
[17] S. Jana, S. Dalapati, M.A. Alam, N. Guchhait, Spectroscopic, colorimetric and theoretical investigation of salicylidene hydrazine based reduced Schiff base and its application towards biologically important anions, Spectrochim. Acta A Mol. Biomol. Spectrosc. 92 (2012) 131–136.
[18] J.L. Kolanowski, F. Liu, E.J. New, Fluorescent probes for the simultaneous detection of multiple analytes in biology, Chem. Soc. Rev. 47 (2018) 195–208.
[19] X. Jiao, Y. Li, J. Niu, X. Xie, X. Wang, B. Tang, Small-molecule fluorescent probes for imaging and detection of reactive oxygen, nitrogen, and sulfur species in biological systems, Anal. Chem. 90 (2018) 533–555.
[20] X. Huang, J. Song, B.C. Yung, X. Huang, Y. Xiong, X. Chen, Ratiometric optical nanoprobes enable accurate molecular detection and imaging, Chem. Soc. Rev. 47 (2018) 2873–2920.
[21] M.R. Filipovic, J. Zivanovic, B. Alvarez, R. Banerjee, Chemical biology of H_2S signaling through persulfidation, Chem. Rev. 118 (2018) 1253–1337.
[22] X. Jin, X. Wu, B. Wang, P. Xie, Y. He, H. Zhou, B. Yan, J. Yang, W. Chen, X. Zhang, A reversible fluorescent probe for Zn^{2+} and ATP in living cells and in vivo, Sensors Actuators B Chem. 261 (2018) 127–134.
[23] M. She, Z. Wang, T. Luo, B. Yin, P. Liu, J. Liu, F. Chen, S. Zhang, J. Li, Fluorescent probes guided by a new practical performance regulation strategy to monitor glutathione in living systems, Chem. Sci. 9 (2018) 8065–8070.
[24] X. Jin, S. Wu, M. She, Y. Jia, L. Hao, B. Yin, L. Wang, M. Obst, Y. Shen, Y. Zhang, J. Li, Novel fluorescein-based fluorescent probe for detecting H_2S and its real applications in blood plasma and biological imaging, Anal. Chem. 88 (2016) 11253–11260.

[25] F. Ding, Y. Zhan, X. Lu, Y. Sun, Recent advances in near-infrared II fluorophores for multifunctional biomedical imaging, Chem. Sci. 9 (2018) 4370–4380.
[26] P. Qu, X. Ma, W. Chen, D. Zhu, H. Bai, X. Wei, S. Chen, M. Xu, A coumarin-based fluorescent probe for ratiometric detection of hydrazine and its application in living cells, Spectrochim. Acta A Mol. Biomol. Spectrosc. 210 (2019) 381–386.
[27] Y. Shen, X. Zhang, Y. Zhang, H. Li, Y. Chen, An ICT-modulated strategy to construct colorimetric and ratiometric fluorescent sensor for mitochondria-targeted fluoride ion in cell living, Sensors Actuators B Chem. 258 (2018) 544–549.
[28] D. Roy, A. Chakraborty, R. Ghosh, Coumarin based colorimetric and fluorescence on-off chemosensor for F^{-}, CN^{-} and Cu^{2+} ions, Spectrochim. Acta A Mol. Biomol. Spectrosc. 191 (2018) 69–78.
[29] G.G.V. Kumar, M.P. Kesavan, G. Sivaraman, J. Rajesh, Colorimetric and NIR fluorescence receptors for F^{-} ion detection in aqueous condition and its live cell imaging, Sensors Actuators B Chem. 255 (2018) 3194–3206.
[30] Q. Yang, C. Jia, Q. Chen, W. Du, Y. Wang, Q. Zhang, A NIR fluorescent probe for the detection of fluoride ions and its application in in vivo bioimaging, J. Mater. Chem. B 5 (2017) 2002–2009.
[31] Y.-C. Wu, J.-Y. You, K. Jiang, J.-C. Xie, S.-L. Li, D. Cao, Z.-Y. Wang, Colorimetric and ratiometric fluorescent sensor for F− based on benzimidazole-naphthalene conjugate: reversible and reusable study & design of logic gate function, Dyes Pigments 140 (2017) 47–55.
[32] M. Nemati, R. Hosseinzadeh, R. Zadmard, M. Mohadjerani, Highly selective colorimetric and fluorescent chemosensor for fluoride based on fluorenone armed calix [4]arene, Sensors Actuators B Chem. 241 (2017) 690–697.
[33] S. Dixit, N. Agarwal, Synthesis of imidazoaryl-BODIPY derivatives for anion sensing applications, J. Photochem. Photobiol. A Chem. 343 (2017) 66–71.
[34] W. Hu, L. Zeng, Y. Wang, Z. Liu, X. Ye, C. Li, A ratiometric two-photon fluorescent probe for fluoride ion imaging in living cells and zebrafish, Analyst 141 (2016) 5450–5455.
[35] Z. Liu, L. Liu, M. Sun, X. Su, A novel and convenient near-infrared fluorescence "turn off–on" nanosensor for detection of glucose and fluoride anions, Biosens. Bioelectron. 65 (2015) 145–151.
[36] G. Nie, Y. Sun, F. Zhang, M. Song, D. Tian, L. Jiang, H. Li, Fluoride responsive single nanochannel: click fabrication and highly selective sensing in aqueous solution, Chem. Sci. 6 (2015) 5859–5865.
[37] Q. Zhao, J. Kang, Y. Wen, F. Huo, Y. Zhang, C. Yin, "Turn-on" fluorescent probe for detection of H2S and its applications in bioimaging, Spectrochim. Acta A Mol. Biomol. Spectrosc. 189 (2018) 8–12.
[38] B. Zhu, M. Zhang, L. Wu, Z. Zhao, C. Liu, Z. Wang, Q. Duan, Y. Wang, P. Jia, A highly specific far-red fluorescent probe for imaging endogenous peroxynitrite in the mitochondria of living cells, Sensors Actuators B Chem. 257 (2018) 436–441.
[39] Y. Wang, L. Wu, C. Liu, B. Guo, B. Zhu, Z. Wang, Q. Duan, Z. Ma, X. Zhang, A highly specific and ultrasensitive fluorescent probe for basal lysosomal HOCl detection based on chlorination induced by chlorinium ions (cl+), J. Mater. Chem. B 5 (2017) 3377–3382.
[40] B. Dong, X. Song, X. Kong, C. Wang, N. Zhang, W. Lin, Two-photon red-emissive fluorescent probe for imaging nitroxyl (HNO) in living cells and tissues, J. Mater. Chem. B 5 (2017) 5218–5224.
[41] X. Jiao, C. Liu, K. Huang, S. Zhang, S. He, L. Zhao, X. Zeng, Molecular design and synthesis of a pH independent and cell permeant fluorescent dye and its applications, Org. Biomol. Chem. 13 (2015) 6647–6653.
[42] K. Dhanunjayarao, V. Mukundam, K. Venkatasubbaiah, Ratiometric sensing of fluoride anion through selective cleavage of SiO bond, Sensors Actuators B Chem. 232 (2016) 175–180.
[43] X. Tian, X. Tong, Z. Li, D. Li, Q. Kong, X. Yang, In vivo fluoride ion detection and imaging in mice using a designed near-infrared ratiometric fluorescent probe based on IR-780, J. Agric. Food Chem. 66 (2018) 11486–11491.